The Effect of Variable Coriolis Parameter in a Planetary Circulation Generated by a Two-Parameter Quasigeostrophic Model[1]

ABRAHAM HUSS

Hebrew University, Jerusalem, Israel

(Manuscript received 23 October 1963, in revised form 24 March 1964)

ABSTRACT

The governing equations of a two-level quasigeostrophic model were integrated twice for periods of about 10 days, once including variation of the Coriolis parameter (the β term) and once excluding it. As expected, the exclusion of the β-term resulted in a quicker rate of development. The evolving perturbation had almost the same pattern in the two cases, but the final distribution of the mean zonal winds was different. In the $\beta=0$ case the zonal velocities in the central region tended towards a barotropic pattern, while a baroclinic jet was formed in the case where $\beta\neq 0$. The numerical integration is also compared with linear theory.

1. Introduction

During a series of experiments for the purpose of studying the generation of general circulation patterns in a planetary atmosphere, it was decided to observe the effect of the "β-term" which represents the effect of the spherical shape of the earth. (Rossby *et al.*, 1939.) By means of linear theory it is comparatively easy to assess the influence of the β-term in simple models at the initial moment of a small amplitude sinusoidal disturbance. However, during prolonged integrations the nonlinear interactions might alter to a certain extent the role of the β-term in the generated circulation pattern.

It was therefore decided to produce two extended numerical integrations, in one of which β was zero. The dynamical model chosen was a two-level geostrophic model very similar to that used by Phillips in his general circulation experiment (1956). To a certain extent this should provide a first step towards a numerical analogue to experiments in rotating heated basins when the spherical effect is absent, as can be seen by comparing the results with the experimental data given by Riehl and Fultz (1957). The computation in which the β-term was retained will be referred to as the "control run."

The prediction equations (Huss and Mintz, 1962) are

$$\frac{\partial q_1}{\partial t}=-\mathbf{v}_1\cdot\nabla q_1 \qquad \frac{\partial q_2}{\partial t}=-\mathbf{v}_3\cdot\nabla q_3 \tag{1}$$

where the potential vorticities, q_1 and q_3, which carry the history of the motion, are

$$\begin{aligned} q_1&=\beta y+\zeta_1-\lambda(\psi_1-\psi_3)=\beta y+\nabla^2\psi_1-\lambda(\psi_1-\psi_3)\\ q_3&=\beta y+\zeta_3+\lambda(\psi_1-\psi_3)=\beta y+\nabla^2\psi_3+\lambda(\psi_1-\psi_3). \end{aligned} \tag{2}$$

All of these symbols have their usual meaning (and are defined in the 1962 paper). Subscripts 0, 1, 2, 3, and 4 refer to the pressure 250, 500, 750, and 1000 mbs, ψ is the streamfunction, and λ is proportional to the static stability. λ had the value 1.261×10^{-12} m^{-2} while β was either zero or 1.6×10^{-11} m^{-1} sec^{-1}. The north-south extent of the region was 6216 km. The equations were solved with centered finite differences, as described in the 1962 paper.

2. Initial conditions

The initial conditions consisted of a basic state on which a perturbation was superimposed. For the initial basic state we assumed that the mean zonal surface wind was zero in all latitudes ($\bar{U}_4=0$), and that the temperature decreased linearly from $T_2=267.4$K at one grid interval distance from the southern boundary to $T_2=219.4$K at one grid interval distance from the northern boundary. This temperature gradient corresponds approximately to the observed temperature gradient in the central latitudes of the northern hemisphere in the winter season. This assumption, together with the boundary conditions, determined the initial ψ-(zonal) average values of ψ_1, ψ_3, q_1 and q_3 at all latitudes. The mean zonal velocity had a value of 8.1 m sec^{-1} at the 750-mb level and 36.0 m sec^{-1} at the 250-mb level (except at grid points adjacent to the southern and northern boundaries, where half these values existed).

Initially the zonally averaged vorticity is zero (except at grid points adjacent to the y-boundaries, where the

[1] This investigation was supported by funds provided by the Geophysics Research Division of the Air Force Cambridge Research Laboratories (Contract AF 19(604)-4963) and by the National Science Foundation (Grant NSF G-14698).

finite differences again introduced a certain discrepancy). Thus, from the point of view of barotropic stability, the initial development will serve as a partial illustration of the considerations raised, for instance, by Kuo (1951). In the experiment with $\beta=0$, the zonally averaged absolute vorticity is identical with the zonally averaged relative vorticity; therefore the stabilizing effect of the variable Coriolis term is absent.

A sinusoidal initial perturbation was superimposed on this basic flow. In some trial runs with the control model ($\beta\neq 0$) three different wavelengths in the x-direction were chosen, corresponding to wavelengths of 12,432 km, 6,216 km and 4,144 km. Appreciable growth, as predicted by linear theory, was found only in the case of the wavelength of 6,216 km, which was therefore adopted for the run with $\beta=0$.

The initial perturbation had identical amplitudes and phase at the 250- and 750-mb levels, so that the isotherms initially were the straight lines given by the basic state alone. The initial perturbation amplitude was small. At the central altitude it corresponded to 9 m in the height of the isobaric surface, and decreased linearly from the central latitude to zero at the northern and southern boundaries. (A test run, in which the amplitude of the initial perturbation varied sinusoidally from the central latitude to the side walls, produced only small differences from the results shown here.)

3. Description of the evolving circulation

The numerical integration was carried for 11 days. While the general features were similar in both runs, considerable differences were found in the rate of the development of the perturbation and in certain structural details.

The development was much more rapid in the case $\beta=0$, as may be seen by comparing Fig. 1 in this paper with the corresponding figure in the control experiment (Huss and Mintz, 1962). After four days in the control experiment, the closed lows and highs at 1000 mb deviated from the mean height of the surface by slightly more than 15 m. The deviation on the same date, in the run with $\beta=0$, was more than 30 m. The isotherms in the $\beta=0$ case also developed larger amplitudes. On the tenth day, the 1000-mb height deviations were 360 ($\beta\neq 0$) and 720 m ($\beta=0$). A considerable noise level in the streamline, temperature and vertical-velocity fields began at that time to obscure the meteorological pattern.

The shape of the disturbance in the central latitude remained approximately sinusoidal (in ψ) for most of the integration. Because of this it could be compared to a linear solution consisting of a basic zonal flow, constant in time, with a superimposed perturbation, having the form:

$$\begin{aligned}\psi_1 &= -U_1 y+\alpha_1(t)\cos my\cos[kx+\sigma t+\delta_1(t)],\\ \psi_3 &= -U_3 y+\alpha_3(t)\cos my\cos[kx+\sigma t+\delta_3(t)],\end{aligned}\tag{3}$$

where U_1, U_3 = the constant zonal velocities at 250 mb and 750 mb, $\alpha_1(t)$, $\alpha_3(t)$ = the amplitudes of the perturbations at 250 mb and 750 mb, $m=2\pi/W$, where W is the wavelength in the y direction, $k=2\pi/L$, where L is the wavelength in the x direction, σ = a phase parameter, having the same value at both levels, $\delta_1(t)$, $\delta_3(t)$ = phase angles, with a different time dependence at 250 mb and 750 mb. The initial conditions adopted require: $\alpha_1(0)=\alpha_3(0)$ and $\delta_1(0)=\delta_3(0)=0$.

A solution, having quite similar features, has been derived by Ogura (1957). Making use of his method, with slight modifications, we obtain, for the general

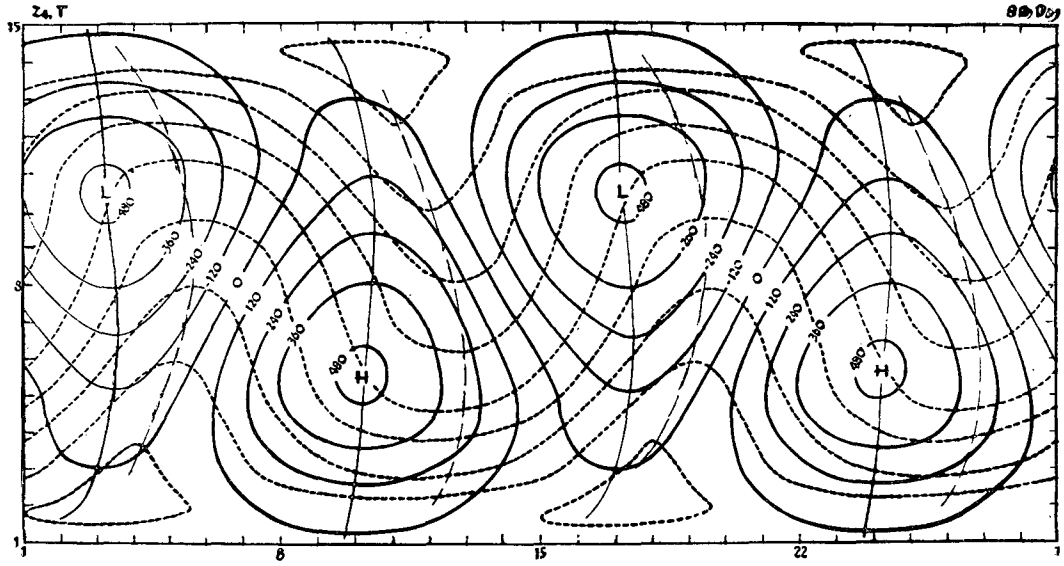

FIG. 1. The circulation on the 8th day; with $\beta=0$. Continuous lines are the height contours of the 1000-mb pressure surface (as deviations from the mean height of the surface in meters). The broken lines show the temperature field, as deviations from the mean temperature of the level in intervals of 5 deg.

case of $\beta \neq 0$:

$$\alpha_1^2(t) = \alpha^2(0)\left\{\cosh^2\tau t + \left[\frac{2B+V(2-\gamma^*)}{E}\right]\sinh^2\tau t\right\}$$
$$\alpha_3^2(t) = \alpha^2(0)\left\{\cosh^2\tau t + \frac{[2B-V(2-\gamma^*)]^2}{E}\sinh^2\tau t\right\} \quad (4)$$

$$\tan\delta_1(t) = \frac{2B+V(2-\gamma^*)}{E}\tanh\tau t$$
$$\tan\delta_3(t) = \frac{2B-V(2-\gamma^*)}{E}\tanh\tau t. \quad (5)$$

The symbols have the meaning

$$\tau = \frac{kE}{2(2+\gamma^*)} \quad (6)$$

$$V = U_1 - U_3 \quad (7)$$

$$B = \frac{\beta}{k^2+m^2}, \quad \gamma^* = \frac{k^2+m^2}{\lambda} \quad (8)$$

$$E = -i[V^2(\gamma^{*2}-4)+4B^2]^{\frac{1}{2}} \quad (9)$$

$$\sigma = \frac{k}{2(2+\gamma^*)}[-(U_1+U_3)(\gamma^*+2)+2B(\gamma^*+1)]. \quad (10)$$

Diagrams illustrating these solutions for the numerical values assumed by us may be found in the paper by Huss and Mintz (1962). The amplitudes and the phase lag $[\delta_1(t)-\delta_3(t)]$ for $\beta=0$, obtained by setting $\beta=0$ in (4)–(10) are given in Figs. 2 and 3, together with the corresponding values, at the central latitude, for the non-linear solution resulting from the numerical integration.

The boundary between the stable and the unstable regime of the linear solution, for variable vertical shear U_1-U_3 and variable wavelength L, is given by $E=0$ for given values of λ and m. With $\beta=0$, waves longer than a certain critical length are unstable for all values of U_1-U_3. When the angular wave number in the y direction is 0, this critical wavelength amounts to 3950 km; with $m=5.897\times10$ radians m^{-1}, corresponding approximately to the meridional variation of amplitude in our experiment, the critical wavelength in the x-direction is 4130 km. Thus the change is quite small. The stabilizing effect in the region of larger wavelengths disappears with the assumption $\beta=0$. With the choice of parameters adopted in our experiment, and with a wavelength of 6216 km, we are well within the unstable region.

In the control experiment with $\gamma^*=1.086$, $[2B+V(2-\gamma^*)]$ will be greater than $[2B-V(2-\gamma^*)]$ and, according to (4), α_3 will increase at a somewhat slower rate than α_1. With $\beta=0$, on the other hand, $\alpha_1(t)$ and $\alpha_3(t)$ are identical.

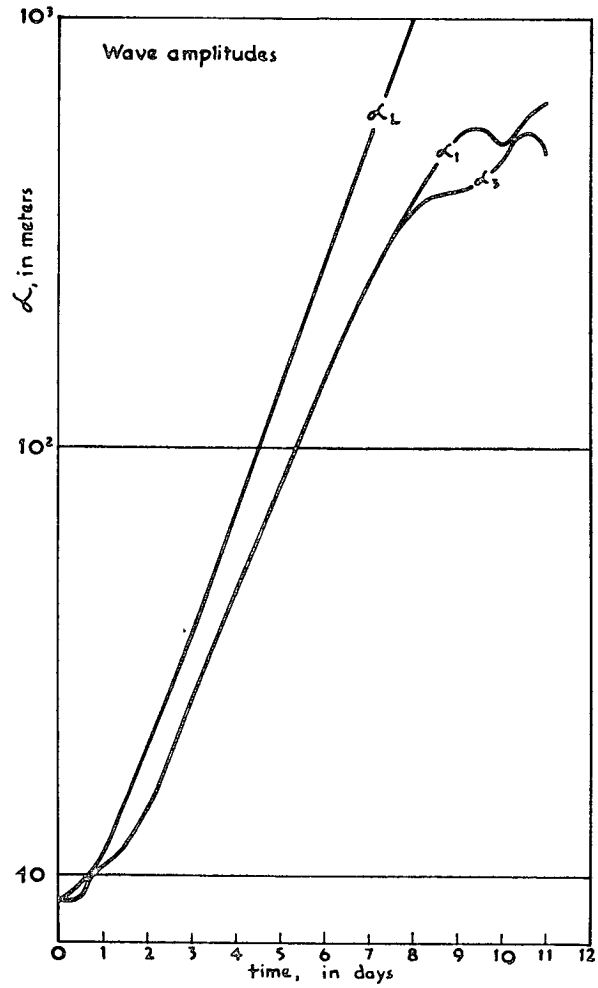

FIG. 2. Wave amplitudes at the central latitude when $\beta=0$. α_1 is at 250 mb; α_3 is at 750; α_L is the solution according to the linear theory in equations (3)–(10).

The actual rate of development in the control experiment ($\beta\neq0$) was somewhat smaller than the rate predicted by linear theory, even during the early stages. After degeneration sets in there is, of course, no correspondence between the two. As expected, the amplitude of the lower wave was found to be smaller than that of the upper wave, both lying below the corresponding values of the linear solution at all times. The phase lag in the control experiment, corresponded quite closely to linear theory until the 8th day.

The variation of the amplitudes and the phase lag when $\beta=0$ is illustrated in Figs. 2 and 3. Linear theory predicts identical values of α_1 and α_3 at all times. The numerically computed values of α_1 and α_3 were lower but nearly identical for about 7 days. (The irregular behavior during the first day may have been caused by the initial conditions.) Following the 7th day the amplitudes, after reaching 308 m began to behave differently

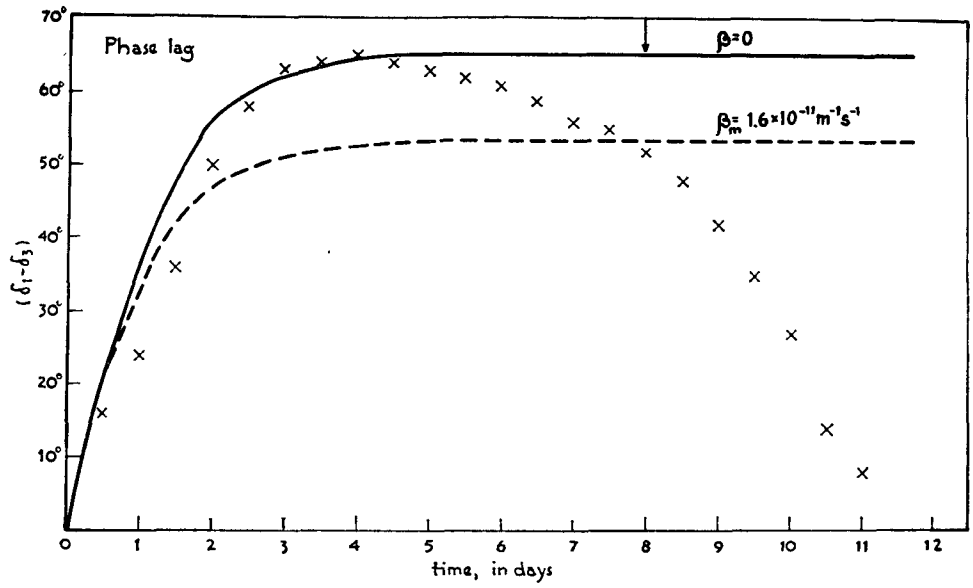

FIG. 3. Phase lags at the central latitude. The crosses show the numerical solution for $\beta=0$; the solid line shows the solution according to linear theory with $\beta=0$; the broken line shows the solution according to linear theory with $\beta=1.6\times10^{-11}$ m^{-1} sec^{-1}.

at the two levels. The amplitude at 250 mb continued to increase up to a maximum of 558 m on the 11th day. In the downward trend of the oscillation a minimum of 502 m was reached, followed again by an increase. The value of the amplitude at 750 mb remained consistently below that of the 250 mb amplitude. It increased at first at a low rate, speeded up to the 9th day and reached a maximum of 557 m on the 10th day, which was followed by a downward trend.

When $\beta=0$, the phase lag between the upper and lower waves followed the curve of linear prediction, with its limiting value of 65°, only for about 4 days. After that it decreased, but no negative values were encountered. It appears that because of the quicker rate of development in this case, the store of available energy became exhausted at an earlier date, and deterioration set in sooner. This would also explain the fact that the greatest amplitudes found in both runs do not differ very much from each other; 593 m in the control run ($\beta\neq0$) and 637 m when $\beta=0$.

Another aspect of the developing circulation is shown by the changes in the mean zonal wind at the central latitude, where the largest velocities were encountered. A comparison of the corresponding values of the two runs is shown in Fig. 4, which has a bearing on Rossby's discussion (1947) on the dynamics of the building up of a zonal wind maximum. The changes in the averaged zonal winds are non-linear effects, brought about by momentum flux divergences and the mean zonal Coriolis force associated with the mean meridional circulation. During most stages of the run these two effects act in opposite direction at the 250-mb level and reinforce each other at the 750-mb level.

With $\beta=0$ we encounter an initial slight decrease in

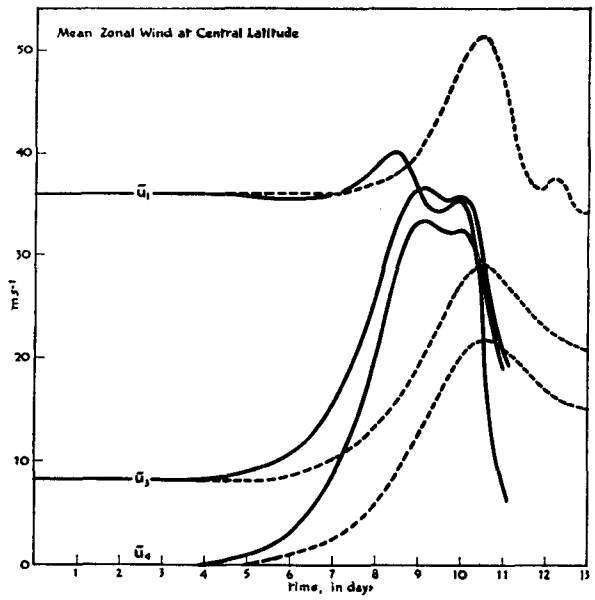

FIG. 4. The mean zonal wind at the central latitude as a function of time, in units of m sec^{-1}. The solid lines are for $\beta=0$; the broken lines are for $\beta=1.6\times10^{-11}$ m^{-1} sec^{-1}.

the mean zonal wind at the 250-mb level, lasting from the last quarter of the 4th day until the beginning of the 7th day, amounting to about 0.4 m sec^{-1} at its extreme. Nothing like that was found in the control run. A maximum of 40 m sec^{-1} was reached after 8½ days—the total increase being no more than 4 m sec^{-1} (or about one quarter of the corresponding increase in the control run). This was followed by an oscillation, with a secondary maximum of 35.5 m sec^{-1} (i.e., somewhat less than the initial value) on the 10th day. The appearance

of the oscillation was similar to the one observed in the control run at a later date. But in this case, after the secondary maximum, the velocity decreased rapidly to a value of 7.7 m on the 11th day—this behavior having, no counterpart in the control run. The variation of U_3 in the $\beta=0$ run was not even approximately in phase with that of U_1—another feature which is different in the two runs. At the 750-mb level the velocity increase was very marked, the greatest value of 36.6 m appearing on the 9th day. This maximum lagged behind the corresponding maximum at the upper level by 12 hours. It was followed first by a very shallow oscillation and then by a rapid downward trend, reaching 20.3 m sec^{-1} at the end of the run (12.2 m sec^{-1} above the initial value). At the beginning of the 9th day the mean zonal velocities became equal, and after that the mean zonal wind velocity at the 750-mb level became greater than the corresponding velocity at the higher level. At the moment of vanishing shear the south-north temperature gradient vanished in the central region, and with the negative shear the poleward temperature gradient was reversed. At the end of the $\beta=0$ run the total temperature contrast between the northern and southern boundaries reached the very low value of 1C. A thorough mixing of the whole model atmosphere has occurred, with a corresponding depletion of zonal available potential energy.

Fig. 5 provides us with a view of the zonally averaged zonal winds at different dates in the $\beta=0$ run. The rapid rate at which the central jet developed is clearly indicated. On the 6th day the central latitudes already showed perceptibly larger velocities. The regions of the low-level easterlies to the north and south were more pronounced in this case than in the control run. A fully developed "jet," with surface westerlies of about 20 m sec^{-1}, and surface easterlies of about 5 m sec^{-1} made their appearance on the 8th day. A similar development occurred in the control run ($\beta\neq0$) only 2 days later. The maximum wind speeds in the core of the "jet" at high altitudes were appreciably higher in the control run (cf. 10th day on Fig. 4), while greater values of velocities in the easterlies were encountered in the run with $\beta=0$. By the 10th day of the run with $\beta=0$, in most of the latitudes the isotachs had a pronounced vertical direction, i.e., the vertical shear of the zonal wind was very small (except near the walls, where, because of the boundary condition, a region of easterlies persisted in the lower half of the model, and a region of westerlies with

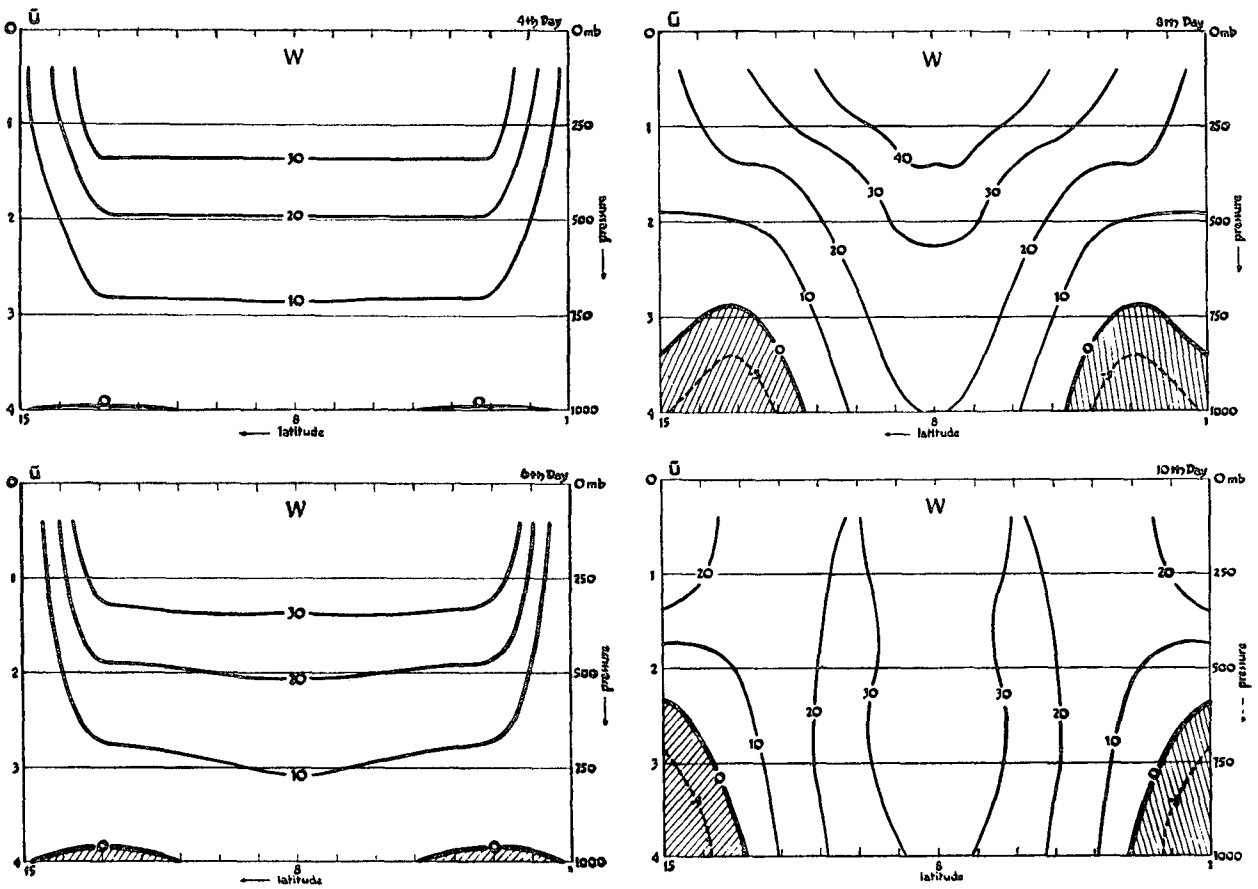

FIG. 5. Meridional cross sections of the zonally averaged zonal winds, in units of m sec^{-1}. The extrapolation at intermediate levels was done according to Mintz (1958).

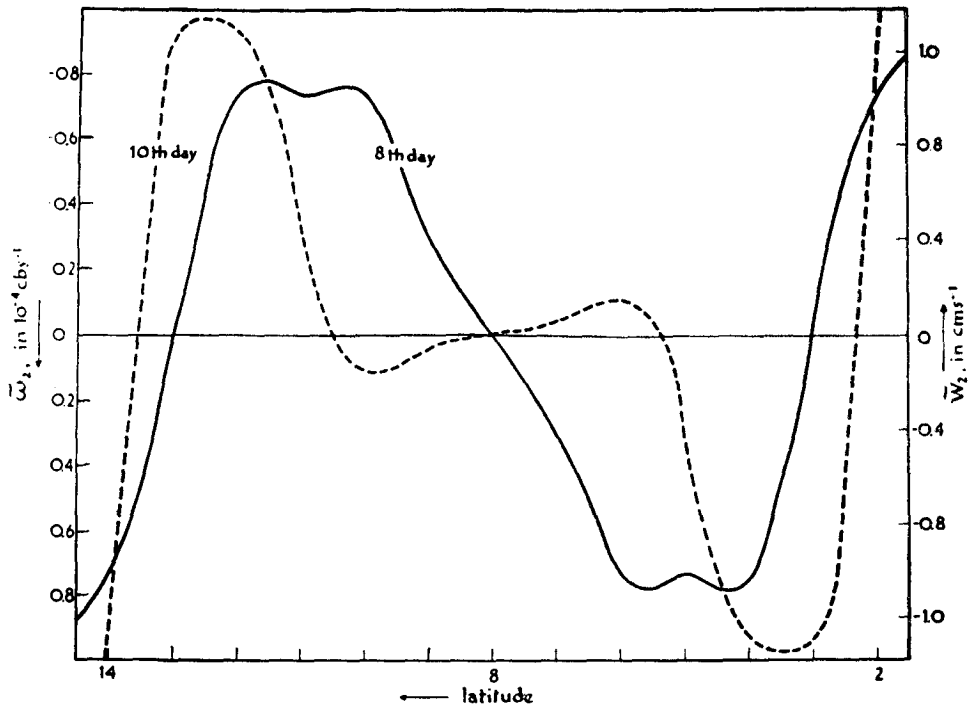

FIG. 6. Zonally averaged values of $\omega \equiv dp/dt$ in units of 10^{-4} cb sec^{-1}, at 8 days and 10 days, when $\beta = .0$

a velocity of about 20 m sec^{-1} above the 500-mb level).

The general features of the meridional circulation in the $\beta=0$ case, developing simultaneously with the changes in the zonal wind distribution, can be seen in the zonally-averaged vertical velocities. Fig. 6 shows their distributions on the 8th and 10th day. On the 8th day, we find three cells, a central "Ferrel" cell, flanked by two "Hadley" cells of equal intensity. During the whole integration time these vertical velocities were consistently higher than in the control run. By the 10th day, there was a 5-cell meridional circulation. E. Eliasen (1961) has shown by linear methods that this might develop from the preceding state due to the presence of certain higher Fourier components in the zonal wind profile and the meridional distribution of the perturbation amplitude. During the latest stages the number of cells rose to 7 (and to 11 in the control run at the beginning of the 12th day, falling off to 5 later on).

Tabulated data obtained during the integration may be found in a report by Huss (1961).

Acknowledgments. The writer is particularly indebted to Prof. Y. Mintz and also wishes to thank Dr. M. S. Rao, Mr. J. Rosenthal and Mr. R. T. Williams, at UCLA, and Mr. G. Assaf at the Hebrew University of Jerusalem, for their assistance and to Mr. D. P. Moore of the Western Data Processing Center and Dr. M. A. Melkanoff, of the Department of Mathematics, UCLA, for help extended in operation of the electronic computer. Computer time on the IBM 709 and IBM 7090 was provided without charge by the Western Data Processing Center of the University of California, Los Angeles.

REFERENCES

Eliasen, E., 1961: On the interactions between the long baroclinic waves and the mean zonal flow. *Tellus*, **13**, 40–55.

Huss, A., 1961: Further studies of the planetary circulation with a quasigeostrophic model. Numerical Studies of Planetary Circulation, Final Report II, Department of Meteorology. University of California, Los Angeles, 30 June 1961.

——, and Y. Mintz, 1962: Growth of a baroclinic wave and evolution of the mean zonal and mean meridional circulations. *Proc. Internat. Symposium on Numerical Weather Prediction* (Tokyo), Meteor. Society of Japan, 539–553.

Kuo, H. L. 1951: Dynamical aspects of the general circulation and the stability of zonal flow. *Tellus*, 3, 268–284.

Mintz, Y., 1958: Design of some numerical general circulation experiments. *Bull. Res. Council Israel: Geo-Sciences*, 7, G, 67–114.

Ogura, Y., 1957: Wave solutions of the vorticity equation for the $2\frac{1}{2}$ dimensional model. *J. Meteor.*, **14**, 60–64.

Phillips, N. A., 1956: The general circulation of the atmosphere: a numerical experiment. *Quart. J. R. meteor. Soc.*, **82**, 123–164.

Riehl, H., and D. Fultz, 1957: Jet streams and long waves in a steady rotating dish-pan experiment: structure of the circulation. *Quart. J. R. meteor. Soc.*, **83**, 215–231.

Rossby, C. G., and collab., 1939: Relation between variations in the intensity of the zonal circulation and the displacement of the semi-permanent centers of action. *J. marine Res.*, 2, 38–55.